Available online at www.sciencedirect.com
SCIENCE DIRECT
Quaternary Research 66 (2006) 1 – 11
QUATERNARY RESEARCH
www.elsevier.com/locate/yqres

A high resolution relative paleointensity record from the Gerlache-Boyd paleo-ice stream region, northern Antarctic Peninsula

Verónica Willmott [a,b], Eugene W. Domack [b], Miquel Canals [a,*], Stefanie Brachfeld [c]

[a] Department of Stratigraphy, Paleontology and Marine Geosciences, University of Barcelona, Barcelona, Spain
[b] Department of Geosciences, Hamilton College, Clinton, NY 13323, USA
[c] Department of Earth and Environmental Studies, Montclair State University, NJ 07043, USA

Received 9 August 2005
Available online 29 March 2006

Abstract

Herein we document and interpret an absolute chronological dating attempt using geomagnetic paleointensity data from a post-glacial sediment drape on the western Antarctic Peninsula continental shelf. Our results demonstrate that absolute dating can be established in Holocene Antarctic shelf sediments that lack suitable material for radiocarbon dating. Two jumbo piston cores of 10-m length were collected in the Western Bransfield Basin. The cores preserve a strong, stable remanent magnetization and meet the magnetic mineral assemblage criteria recommended for reliable paleointensity analyses. The relative paleomagnetic intensity records were tuned to published absolute and relative paleomagnetic stacks, which yielded a record of the last ~8500 years for the post-glacial drape. Four tephra layers associated with documented eruptions of nearby Deception Island have been dated at 3.31, 3.73, 4.44, and 6.86 ± 0.07 ka using the geomagnetic paleointensity method. This study establishes the dual role of geomagnetic paleointensity and tephrochronology in marine sediments across both sides of the northern Antarctic Peninsula.

Keywords: Relative paleomagnetic intensity; Teprhocrhonology; Holocene; Antarctic Peninsula

Introduction

Application of radiocarbon dating in Antarctica is complicated by large reservoir corrections and the limited supply of calcite and algal organic matter suitable for AMS ^{14}C dating. Some depositional systems have provided accurate and reliable ^{14}C chronologies, for example the Palmer Deep (Domack et al., 2001), as evidenced by the smooth progression of ages with depth, the absence of age reversals, and the ability to derive a reproducible reservoir correction factor from surface sediments and calcitic organisms living near the sediment–water interface. However, not all stratigraphically important sequences satisfy these conditions. Many sediment sequences from the Antarctic continental shelf lack biogenic calcite due to cold bottom water temperatures, which enhances dissolution of calcium carbonate. This necessitates the use of the acid insoluble organic matter fraction (AIOM) for ^{14}C dating. However, the AIOM may be affected by reworking, vital effects, and diagenetic effects. In addition, there is a documented spatial and temporal variation in the ^{14}C reservoir correction factor around the Antarctic margin (Andrews et al., 1999; Björck et al., 1991b; Brachfeld et al., 2003; Domack et al., 1999; Gordon and Harkness, 1992; Harden et al., 1992; McMillan et al., 2002; Morgenstern et al., 1996; Van Beek et al., 2002). These complications, while not insurmountable, have motivated the investigation of alternate correlation and dating methods.

Successful studies have been carried out in the Antarctic Peninsula using tephrochronology (Björck et al., 1991a; Palmer et al., 2001; Smellie, 1999), and radioisotopes (Berkman and Ku, 1998; Van Beek et al., 2002). Yet these methods also have limitations, for example the spatial limitations of volcanigenic sources and the need for the appropriate mineralogy and geochemical conditions to preserve radioisotopic carriers in significantly thick sedimentary units.

* Corresponding author.
E-mail address: miquelcanals@ub.edu (M. Canals).

0033-5894/$ - see front matter © 2006 University of Washington. All rights reserved.
doi:10.1016/j.yqres.2006.01.006

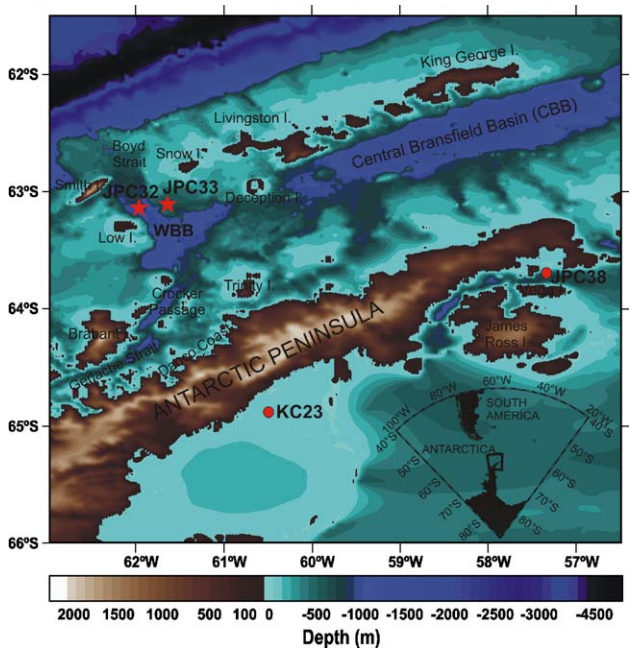

Figure 1. Location map of the Gerlache Strait and Western Bransfield Basin – WBB – area, north Antarctic Peninsula region, constructed from the GEBCO digital database (IOC et al., 2003). Stars show coring sites in this study. Bold points show nearby reference sites used in this work.

Dating based on geomagnetic paleointensity is a proven technique based on tuning paleointensity patterns with a well-dated reference curve, a technique similar to tuning based on oxygen isotope stratigraphy. Paleointensity dating is attractive as long as the reference curve is high resolution, high quality, and independently dated. In the last 10 years, relative paleointensity (RPI) curves have been increasingly used as global, millennial-scale correlation and dating tool (Brachfeld et al., 2003; Channell et al., 2000; Guyodo and Valet, 1996, 1999; Laj et al., 2000; Stoner et al., 2002). This method is particularly attractive in the Antarctic and sub-Antarctic, given the lack of calcite for oxygen isotope stratigraphies and the frequent absence of materials appropriate for radiocarbon dating (Brachfeld et al., 2003; Channell et al., 2000; Mazaud et al., 2002; Sagnotti et al., 2001; Stoner et al., 2002).

This study presents a Holocene RPI record derived from two sediment cores from the western Bransfield Basin (WBB). Once placed on a common depth scale (via correlation of tephra layers identified in each core and correlation of each core's paleointensity records) the WBB relative paleointensity stack is tuned to two reference curves. The reference curves used in this work are ABSINT, a global compilation of >2000 archeomagnetic measurements (Laj et al., 2002; Yang et al., 2000), and an ultra high-resolution sedimentary paleointensity record from the St. Lawrence Estuary (St-Onge et al., 2003). The resulting chronology provides an approximated date for deglaciation of the outer end of the Boyd-Gerlache Strait paleo-ice stream, a major drainage path for glacial ice that once flowed off an expanded Antarctic Peninsula Ice Sheet (Canals et al., 2000).

Materials and methods

Located in the northern Antarctic Peninsula, the Western Bransfield Basin (WBB) is one of three sub-basins that constitute the north-east oriented Bransfield Basin (Fig. 1). This basin is occupied by a morphosedimentary bundle structure made of subparallel ridges and grooves 40 m high and 1–3 km wide that are oriented in a north-west direction (Canals et al., 2000). The WBB bundle documents the presence of a Last Glacial Maximum paleo-ice stream of 340 km length that drained the Gerlache Strait and WBB (Canals et al., 2000). Echo-character mapping of the WBB returned an opaque basal reflector draped by acoustically laminated sediments (Canals et al., 2000; Willmott et al., 2003), suggesting that the drape is made mostly of pelagic and hemipelagic material. A jumbo piston corer (JPC) lined with 10-cm-diameter polyvinyl chloride (PVC) tubes was used to collect two sediment cores in the WBB, during the austral summer of 2000–2001, on board the R/V *Nathaniel B. Palmer*. Two kasten (gravity) cores were collected from each of the two locations in order to capture and correlate the longer JPC cores with an undisturbed modern surface. The locations, length and water depths of the cores are summarized in Table 1. Core JPC-33 was partially lost below 9 m during the recovery process. For that reason, magnetic parameters presented here extend from 0 to 6 m core depth, which is the maximum depth that can be correlated with JPC-32. The dominant lithology recovered at both core sites is a diatom-bearing sandy mud. Chirp data obtained at sites JPC-32 and JPC-33 during the coring process showed 25 m of hemipelagic sediment (Fig. 2).

In order to assess the reliability of these sediments for a geomagnetic paleointensity study, we undertook a detailed investigation of the bulk sediment grain size and the magnetic properties of the sediment. The cores were sampled via u-channels at the Antarctic Marine Geology Research Facility, in Tallahassee, USA, and measured at the Laboratoire des Sciences du Climat et de l'Environment (LSCE) in Gif-sur-Yvette, France. The u-channels were measured on a 2G model 755-R cryogenic magnetometer with DC SQUIDS and in-line alternating field (AF) demagnetization unit. Natural remanent magnetization (NRM) was measured and stepwise AF demagnetized at 0, 5, 10, 15, 20, 25, 30, 35, 40, 45, 50, 55 and 60 mT. Anhysteretic remanent magnetization (ARM) was acquired in a peak alternating field of 100 mT and a steady bias field of 50 μT at a translation speed of 1.0 cm/s. Isothermal Remanent Magnetization (IRM) was acquired in pulsed fields of 0, 50, 100, 200, 300, 500 mT up to 1-T. Back-field IRM was imparted with a DC field of −0.3 T ($IRM_{-0.3\ T}$). Volume-normalized susceptibility (k) was measured with a Bartington MS2C 45

Table 1
Location, lengths and water depth of NBP01-07 JPC-32 and JPC-33

Core	Latitude (°S)	Longitude (°W)	Length, m	Water depth, m
JPC-32	63° 08.014	61° 55.361	8.90	888 m
JPC-33	63° 08.120	61° 29.457	9.05	704 m

JPC: Jumbo Piston Core.

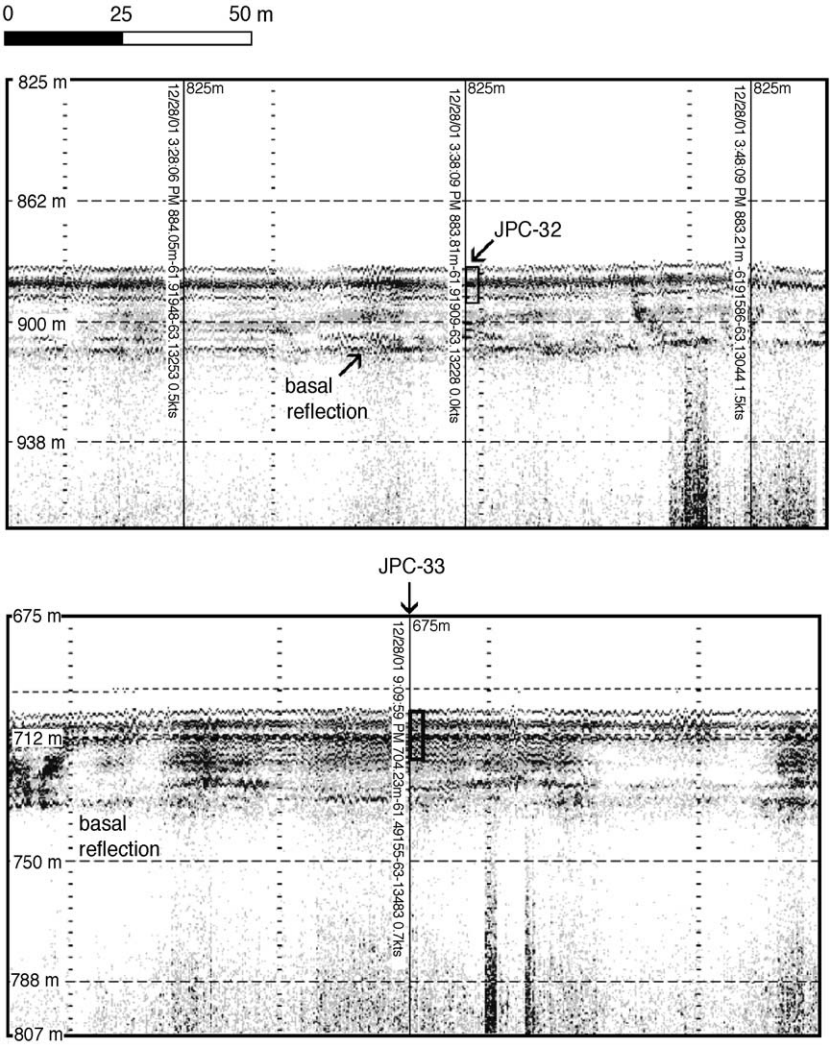

Figure 2. 3.5 kHz Chirp seismic reflection profiles collected at sites JPC-32 and JPC-33 (Ocean Data bathy 2000 W system). The basal reflection is the contact with glacial diamicton.

mm-diameter susceptibility bridge. Subsamples for bulk sediment grain size analysis were collected every 5 cm and analyzed with a Coulter LS 100 laser diffraction particle size analyzer in the University of Barcelona. Spectral analysis and coherence tests were performed on the paleomagnetic data set using the Analyseries software (Paillard et al., 1996) according to methods described by Tauxe and Wu (1990).

Results

Lithology and magnetic properties

Cores JPC-32 and JPC-33 consist of an olive grey, homogeneous, silt-bearing, bioturbated mud, interrupted by four volcaniclastic sands characterized by sharp basal contacts, loading structures, and normal grading. These volcaniclastic sands are interpreted as ash layers. The four ashes were identified and correlated in each core by visual inspection and by their magnetic parameters. The presence of ash layers is very helpful for correlating the lithologic profiles because they were deposited instantaneously and serve as chronostratigraphic markers.

Homogeneity of the magnetic mineral assemblage within a sediment sequence with respect to magnetic concentration, grain size, and mineralogy are criteria that are used to determine whether sediments reliably record the geomagnetic field, or if directional and intensity features result from lithological artifacts. More than 95% of the intensity of the isothermal remanent magnetization in both cores was acquired with fields lower than 300 mT, suggesting that magnetite is the dominant magnetic mineral present (Fig. 3). *S*-ratio values range from 0.94 to 0.98 in the olive grey mud, also consistent with magnetite. The *S*-ratio values drop down to 0.80–0.88 in the ash layers, suggesting the presence of high-coercivity minerals in the tephra layers (Fig. 3). The tephra layers are coarser-grained, a general characteristic for volcanic ashes also reported by Peng and King (1992).

We examined both the bulk sediment grain size and the magnetic "grain size" (Fig. 3). The sediments are dominated by the silt-size fraction, with the exception of the 4 volcanic ash

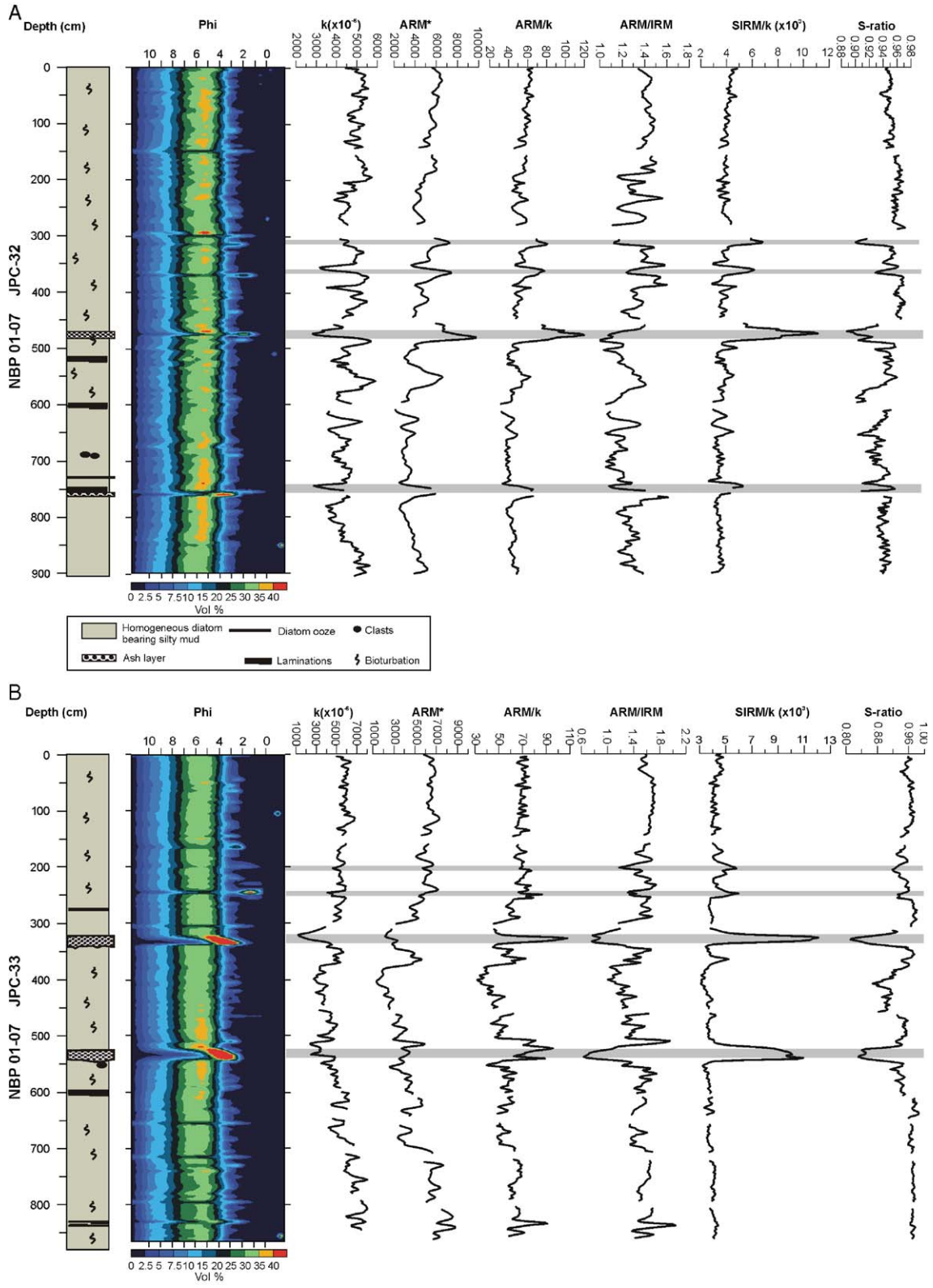

Figure 3. Lithostratigraphy, grain size distribution, magnetic susceptibility, and magnetic parameters (ARM*, ARM/k, ARM/IRM, SIRM/k and *S*-ratio) for core JPC-32 (A) and for core JPC-33 (B).

layers. Exclusive of the ash layers, concentration-dependent magnetic parameters such as k and ARM vary by less than a factor of 3. Susceptibility decreases in the ash layers, whereas ARM increases. Consequently, the magnetic particle size ratio ARM/k shows peaks, but a second magnetic particle size ratio, ARM/IRM, shows low values associated with the ash layers

(Fig. 3). Given the drop in *S*-ratio associated with the ashes, we interpret these seemingly contradictory observations as reflecting a mineralogy change in the ash, rather than reflecting magnetic grain size. We speculate that the ashes contain a high coercivity phase such as (titano)hematite, which would cause low k when measured in a weak applied field, but acquire a high-amplitude IRM in a strong pulsed field. Although the ashes are coarser-grained, titanohematite undergoes magnetic domain state transitions at larger grain volumes than magnetite (Dunlop, 1997). Hypothetically, if this mineral is present in the ash, it would likely be in the stable single domain size range, which would account for all of the observed features in k, ARM/k, ARM/IRM, *S*-ratio, and SIRM/k. With the exception of the ash layers, ARM/k, ARM/SIRM, and *S*-ratio are constant and do not contain any evidence of variations in the mineralogy or grain size of magnetic minerals.

Directional data

Vector-endpoint demagnetization diagrams (Fig. 4) are characterized by a strong, stable, single-component NRM, which decreases linearly towards the origin. In some samples, a soft viscous component was present and was easily removed after the 5- or 10- mT demagnetization level. The median destructive field (MDF) of the olive-grey mud is 20 mT. Unstable demagnetization behavior was detected in the ash layers (Fig. 4), likely due to the change in magnetic mineralogy. The inclination values of the postglacial sediments of both cores fluctuate between the present-day inclination at the site latitude (−56°) and the geocentric axial dipole value of −76. The declinations determined from AF demagnetization were adjusted by a constant factor such that the resulting mean declination of the directionally stable zone was 0 (Fig. 5).

Relative Paleointensity (RPI)

Normalization method

The ash layers were removed from the stratigraphy in order to obtain a shortened depth. For each normalization parameter we calculated the average ratio of NRM/normalizer at the 20, 25, 30 35 and 40-mT demagnetization levels (Fig. 6). The three normalization methods yield similar profiles, only varying in the amplitudes of peaks and troughs. We tested the coherence of the normalized intensity and normalization parameters, NRM/k and k, NRM/ARM and ARM, and NRM/SIRM with SIRM. The best normalization parameter is the one that shows no coherence with its normalizer parameter (Tauxe, 1993; Tauxe and Wu, 1990). At the 95% confidence level the NRM/ARM normalized intensity is not coherent with the normalizer except at periods corresponding to 385, 155, 131 and 119 years for JPC-32 and to 240 and 115 years for JPC-33. NRM/IRM and NRM/x are more strongly coherent with their normalizers and display coherence across a wider band of frequencies (Fig. 7). Therefore, we used ARM as our normalization parameter in both cores.

Correlation between cores was done in two steps. First we used the Keller et al. (2003) geochemical identification

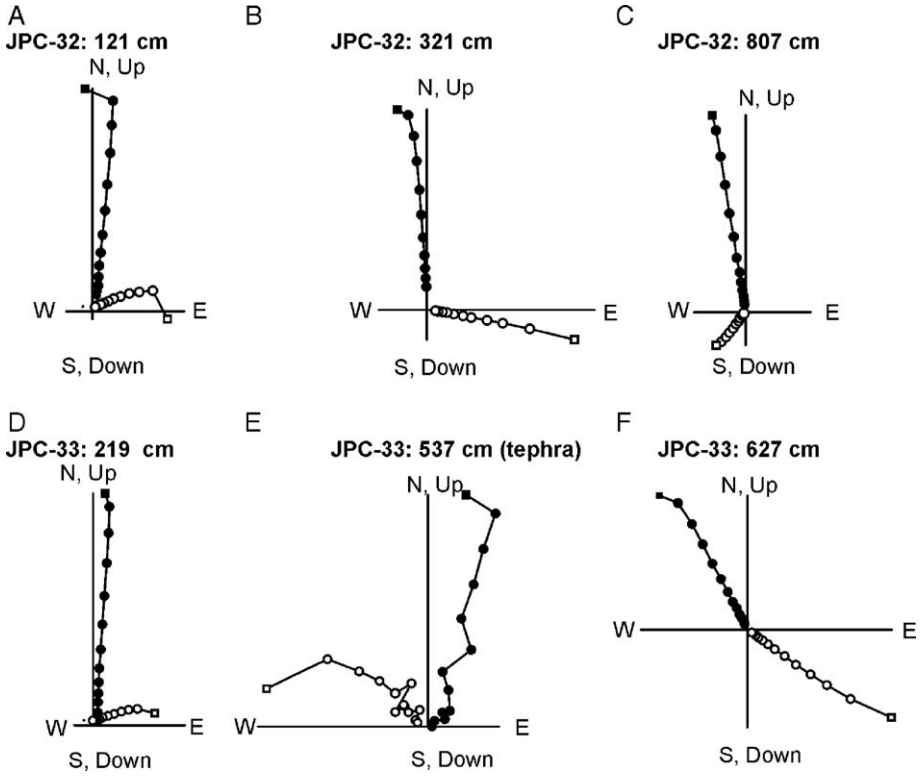

Figure 4. Modified Zidjerveld progressive demagnetization diagrams of typical samples. Solid (open) circles denote projections on the horizontal (vertical) plane. Field steps are 0, 5, 10, 15, 20, 25, 30, 35, 40, 45, 50, 55 and 60 mT. (A) JPC-32, 121 cm depth; (B) JPC-32, 321 cm; (C) JPC-32, 807 cm; (D) JPC-33, 219 cm; (E) JPC-33, 537 cm; (F) JPC-33, 627 cm.

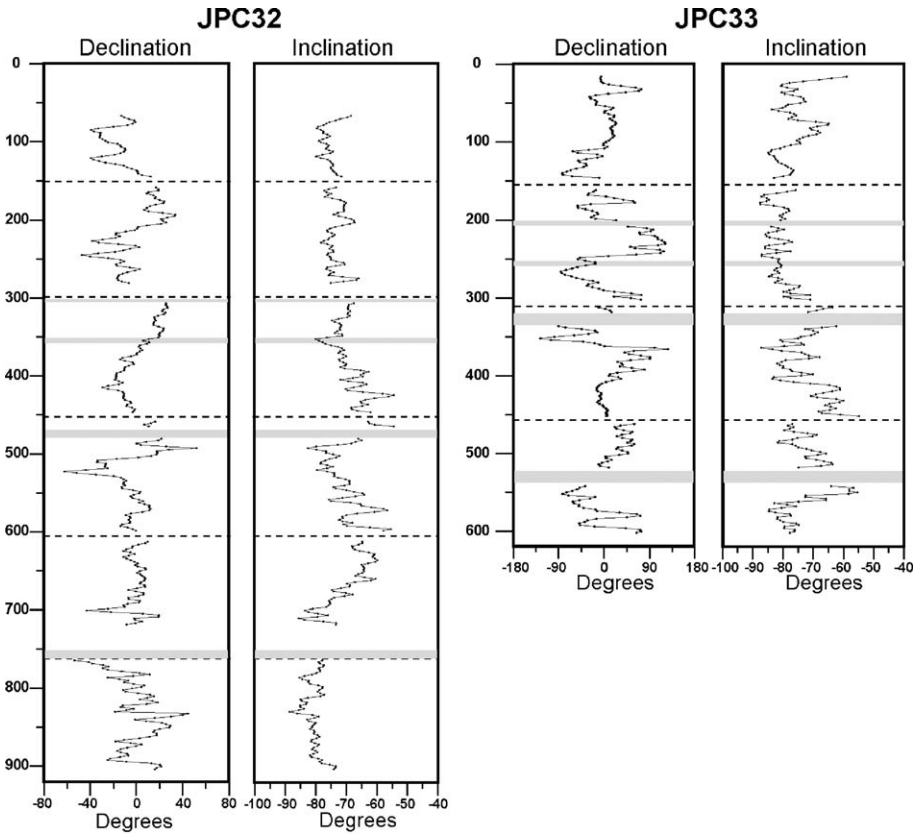

Figure 5. Declination and inclination determined from AF demagnetization at 20 mT. Declinations have been rotated to obtain a whole-core average value of 0°. Dashed horizontal lines indicate core section boundaries. Grey horizontal lines indicate position of ash layers.

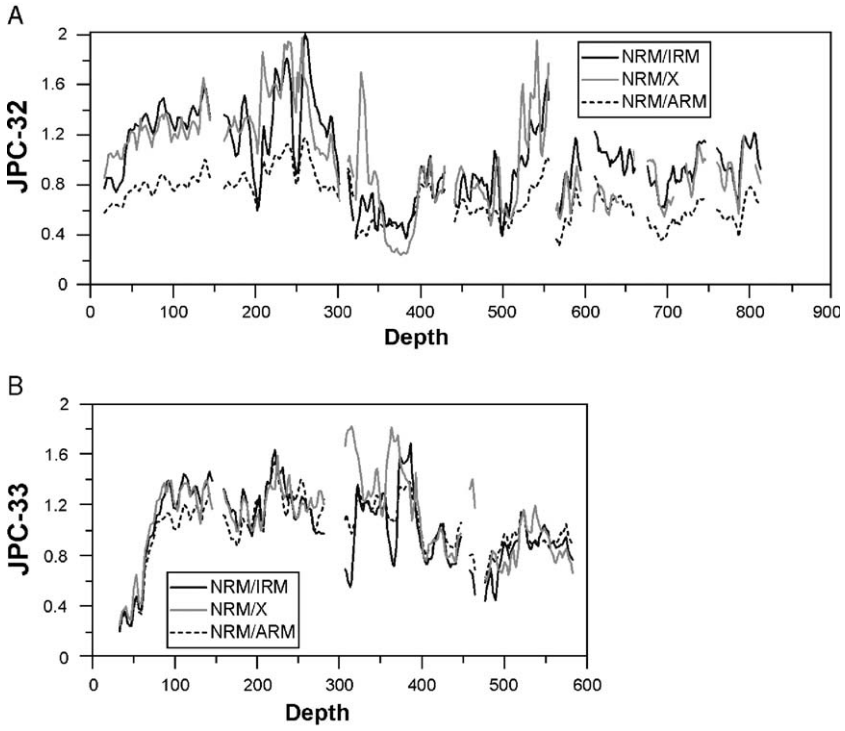

Figure 6. NRM/IRM, NRM/x and NRM/ARM in (A) core JPC-32 and (B) core JPC-33.

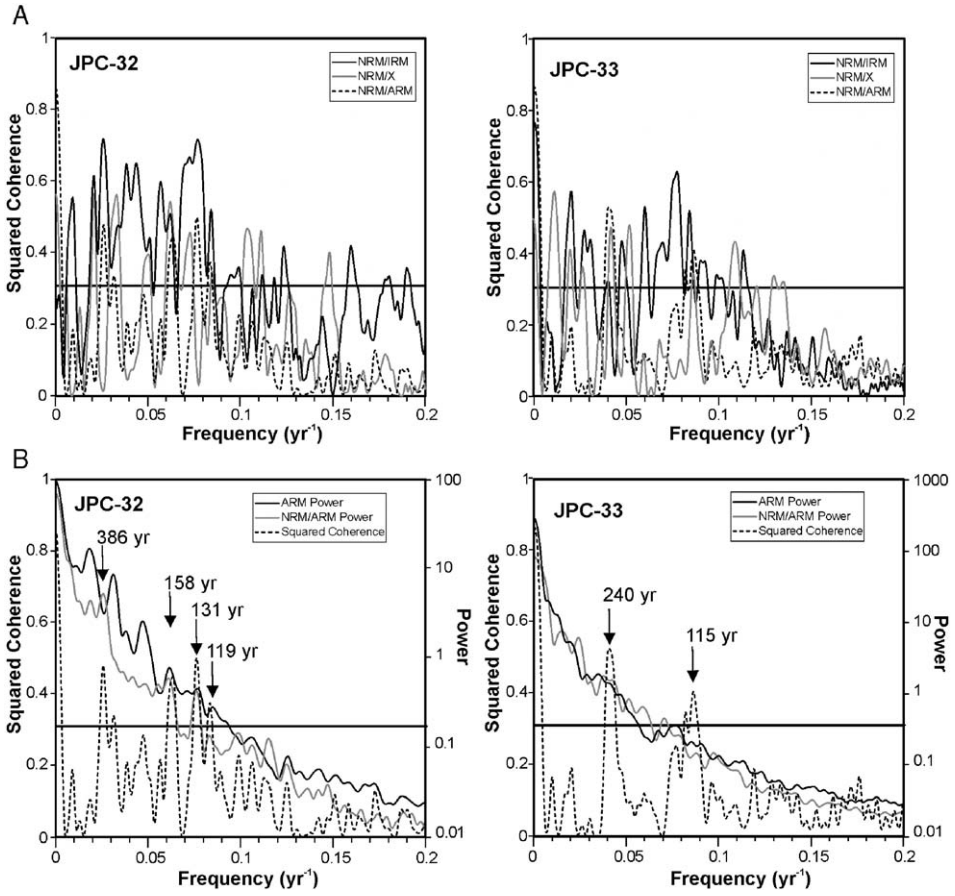

Figure 7. (A) Coherence tests of normalized intensity with the normalization parameters for JPC-32 and JPC-33. (B) Coherence test of normalized intensity and power spectra of ARM and NRM/ARM for cores JPC-32 and JPC-33. The solid horizontal line is the level above which squared coherence is considered significant at the 95% level.

of the ash layers. Keller et al. (2003) matched the ash layer at 470 shortened-cm in JPC-32 with the ash at 330 shortened-cm in JPC-33, and the ash at 760 shortened-cm in JPC-32 correlates with the ash at 530 shortened-cm in JPC-33. The ashes were held as fixed references points that were not allowed to shift position. We then used relative paleointensity (RPI) to adjust the scale of JPC-33 to the scale of JPC-32, the chosen master core (Fig. 8). The alignment of the major peaks and troughs in the NRM/ARM logs is shown in Figure 8A.

Discussion

Relative paleointensity tuning

We used a 2-step tuning process to derive an age model for the WBB cores. First, we tuned the WBB relative paleointensity stack (WBB RPI) to an absolute paleointensity compilation termed ABSINT (Laj et al., 2002; Yang et al., 2000). The two records display similar trends (Fig. 9A). The WBB RPI stack records the decay in geomagnetic field strength over the past ~1000 years. The WBB RPI record displays overall higher intensity in the late Holocene and lower intensity during the middle Holocene. The WBB RPI stack displays three intensity peaks during the late Holocene (0–4 ka), and a 4th smaller peak that immediately follows the middle Holocene low (4–5 ka). These features have wavelengths of 0.75–2 kyr. These features are smoothed out in the ABSINT record due to the data binning and smoothing inherent in its construction. However, these 4 features are clearly seen in other globally distributed data sets including an absolute intensity record from Syria (Genevey et al., 2003), the Larsen Ice Shelf region (Brachfeld et al., 2003), and the St. Lawrence Estuary (St-Onge et al., 2003). Indeed, the WBB RPI stack and the St. Lawrence Estuary Stack appear to have correlative features with wavelengths of <1000 years (Fig. 9B). Therefore, we applied a second tuning by matching intensity peaks and troughs in the WBB RPI record to the St. Lawrence Estuary record, which is independently dated by 17 AMS ^{14}C dates on biogenic calcite (St-Onge et al., 2003). Our resulting geomagnetic paleointensity based age model (Fig. 10) yields an average sedimentation rate of ~1 m/kyr for the Holocene sequence in the Boyd Strait region, consistent with the recent (ca. 100 yr) sediment accumulation rates observed in bottom sediments from the Western Bransfield Basin (Isla et al., 2004; Masque et al., 2002) ranging from 0.52 mm yr^{-1} to 1.56 mm yr^{-1}. Our constructed age model gives a date of 8500 yr for the base of the core. However, the occurrence of higher rates of sedimentation near the drape base and just above the till unit

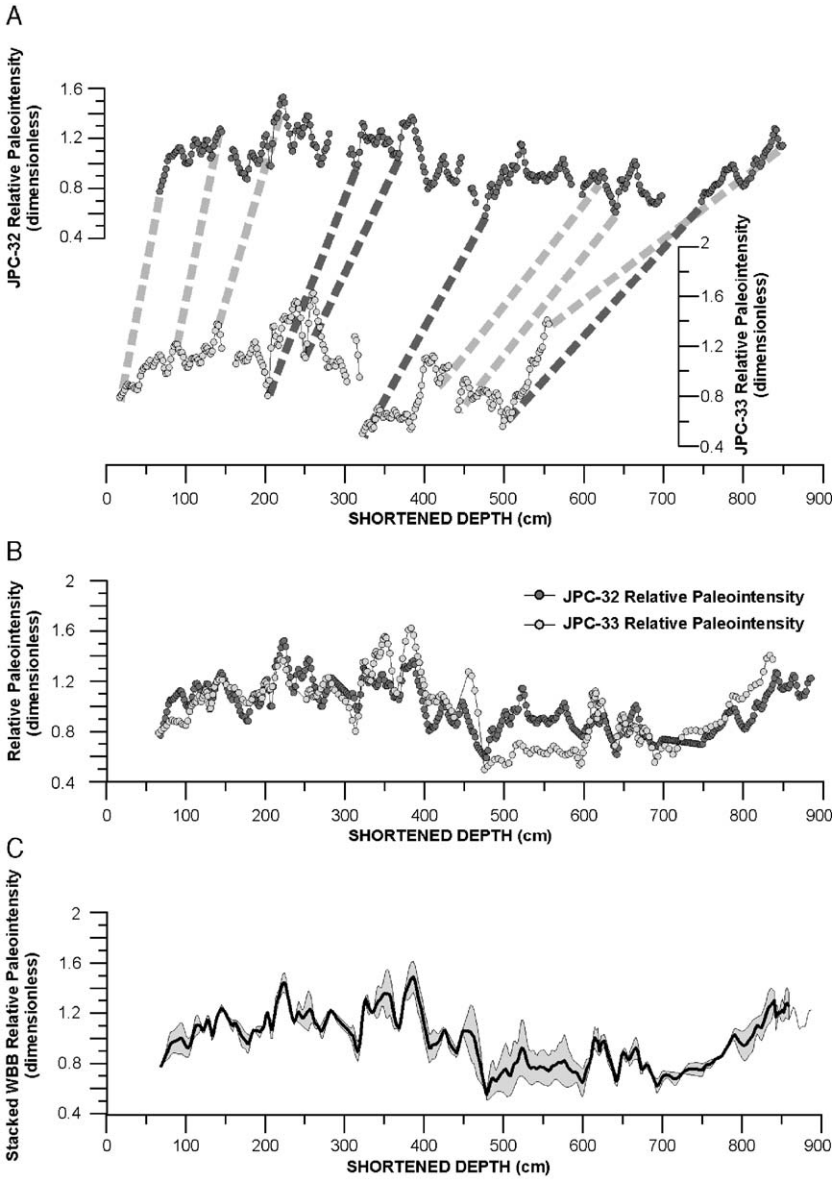

Figure 8. (A) Relative paleointensity logs from cores JPC 32 and JPC 33 vs. shortened depth. Some correlation tie lines are shown. Dark dotted lines indicate correlation between ash layers. (B) Common depth for JPC-32 and JPC-33 after correlation. (C) Stacked RPI vs. common depth. The standard deviation is shown by the grey shaded region.

that might suggest and age close to the accepted Pleistocene to Holocene transition (i.e., 11 ly) (Domack et al., 2001; Pope and Anderson, 1992; Pudsey et al., 1994) as the timing of deglaciation of the outer Boyd-Gerlache Strait paleo-ice stream remains speculative. Further work on sediment cores reaching the very base of the glacial drape is required to sort this point.

Relative paleointensity and tephrochronology

A total of 18 tephras have been identified in late Holocene lacustrine, marine, and terrestrial records across the northern Antarctic Peninsula (Björck et al., 1991c; Matthies et al., 1990; Smellie, 1999). The use of these tephras as chronostratigraphic markers has been limited by the lack of absolute age dates for the majority of these tephras, and incomplete geochemical fingerprinting. Fourteen of these tephras, designated AP1 to AP14, were captured in a moss bank and in 5 lakes from the Northern Antarctic Peninsula and South Shetland Islands (Björck et al., 1991c). Björck et al. (1991b, 1991c) and Smellie (1999), summarized the available absolute age data, most of which came from radiocarbon dating of the moss bank and bulk lacustrine sediment. Björck et al. (1991b, 1991c) noted several complications in the lacustrine radiocarbon dates, including contamination of the radiocarbon pool by old carbon derived from bedrock, penguin guano, and ice/snow melt, or sediment disturbance in shallow lakes due to bottom freezing or oxidation of surface sediments during periods of desiccation (Björck et al., 1991b). Therefore, the lacustrine dates may not provide the best age constraints for the tephras. Björck et al. (1991b) further noted that while the moss bank ages were very robust, the available data extended only from 1600 to 5000 ^{14}C yr B.P.

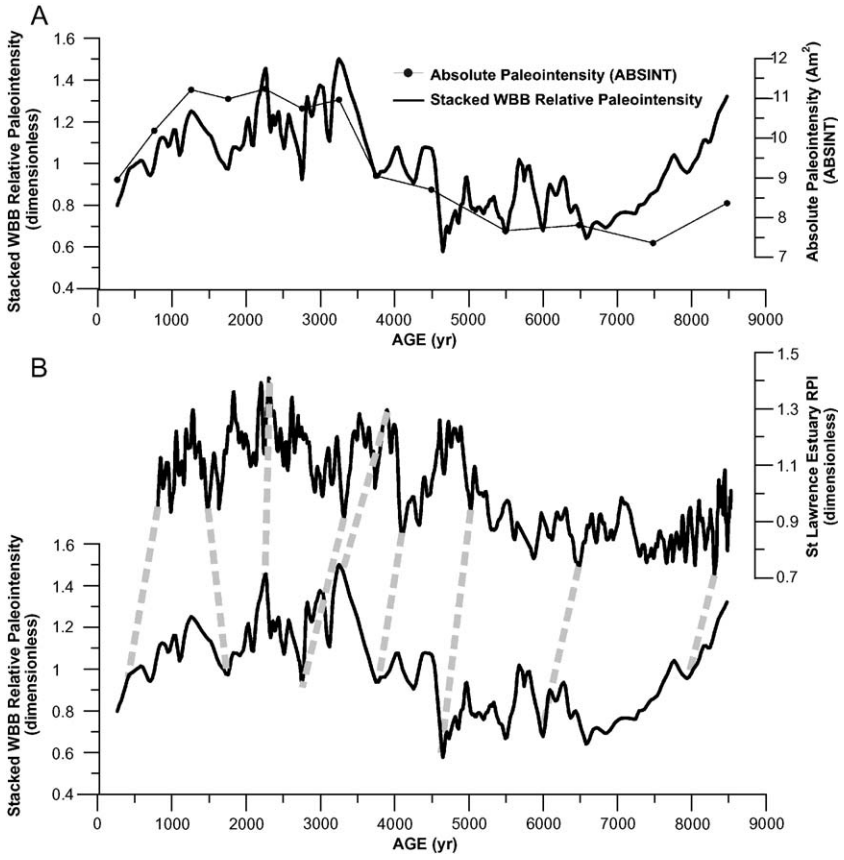

Figure 9. (A) Preliminary composite age model for the WBB master core vs. the ABSINT record. (B) Correlation with the St. Lawrence Estuary RPI. Some correlation tie lines are shown.

The paleointensity study presented here and a parallel study of tephra geochemistry (Keller et al., 2003) can be combined to increase the applicability of tephrochronology in the Antarctic Peninsula region and provide age control back to 8500 yr ago. The four ashes found in JPC-32 and JPC-33 are likely some of the 18 tephras found across the Northern Antarctic Peninsula region (Björck et al., 1991a; Smellie, 1999). The ash located at 530 cm in JPC-33 was identified as a Deception Island tephra, which is recognized as far as 190 km to the east-southeast. The Deception Island tephra was also identified in core NBP00-03 JPC38 from the Vega Drift, northern Prince Gustav Channel, Weddell Sea, which has a preliminary ^{14}C date available based on biogenic calcite (Keller et al., 2003). Keller et al. (2003) conducted an electron microprobe analysis of glass shards from the Vega Drift Deception Island tephra to match the tephra's composition to Deception Island. The Vega Drift Deception Island tephra has an approximate age of 6500 ^{14}C yr B.P. (Keller et al., 2003). However, this date from the Vega Drift was calculated via linear interpolation between two radiocarbon dates of pelecypod shells, which were located 12 m apart in core JCP38 (Drake, 2002; Keller et al., 2003; Lichtenstein et al., 2002). Therefore, we view the Vega Drift ^{14}C date as external

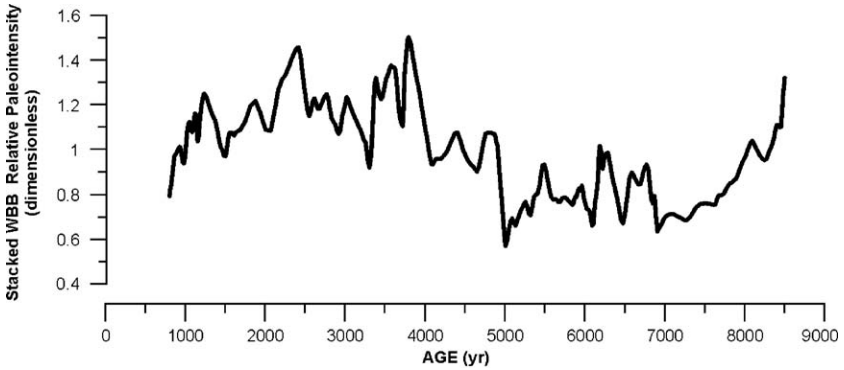

Figure 10. Composite age model for the WBB master core, after correlation with the St. Lawrence Estuary RPI.

check on our paleointensity chronology, but do not use it as the final accepted age of the Deception Island tephra.

Our geomagnetic paleointensity age model enables us to assign ages to the 4 ashes found in JPC-32 and JPC-33. Based on paleointensity tuning to ABSINT and the St. Lawrence Estuary records, we obtained the following ages:

WBB 1 at 310 shortened-cm = 3.31 ± 0.07 ka
WBB 2 at 365 shortened-cm = 3.72 ± 0.07 ka
WBB 3 at 470 shortened-cm = 5.00 ± 0.07 ka
WBB 4 at 760 shortened-cm = 6.92 ± 0.07 ka

The age uncertainty of 70 years is taken from the average uncertainty in the 17 AMS ^{14}C dates on which the St-Onge et al. (2003) record is based. These dates circumvent the problems of the absence of appropriate material for radiocarbon dating, variable reservoir ages, sediment reworking, and variations in the origin of carbon input. When the geochemical profiles of each of these 4 ash layers are completed, the WBB ashes can be used to import our paleointensity ages to other records via geochemical fingerprinting.

Conclusions

Two sediment cores collected from the Boyd Strait, Western Bransfield Basin satisfy the criteria for magnetic uniformity and record a strong, stable remanent magnetization. We normalized the natural remanent magnetization with anhysteretic remanent magnetization in order to construct a relative paleointensity record. The 2 cores were combined on a shortened-cm scale then tuned to the global ABSINT absolute intensity curve (Laj et al., 2002; Yang et al., 2000), followed by tuning to the St. Lawrence Estuary relative paleointensity record (St-Onge et al., 2003). Paleointensity features with wavelengths of <1000–2000 years can be recognized and correlated between the WBB and St. Lawrence Estuary records, suggesting the potential for sub-millennial-scale correlation of geomagnetic paleointensity features. The resulting age model is not conclusive enough to firmly state that the base of the hemipelagic drape in the Boyd-Strait is 11, 000 yr old, and therefore caution is needed before assigning such timing to the deglaciation of the outer Boyd-Gerlache paleo-ice stream region. Using the paleointensity-based chronology, we assign ages of 3.3, 3.7, 5 and 6.9 ka to the 4 tephra layers identified in the WBB cores. In the future, geochemical fingerprinting of these tephras can be used to import our paleointensity-based ages to other sites across the Northern Antarctic Peninsula region.

Acknowledgments

We cordially thank the crew of R/V *Nathaniel B. Palmer*, Raytheon Polar Services technicians, and the science staff of cruise NBP01-07, and Antarctic Marine Geology Research Facility staff members Tom Janecek and Matthew Curren for their help in sampling, description and core logging of the sediment cores. We sincerely thank Drs. Carlo Laj and Catherine Kissel for their generosity, use of the paleomagnetic facilities at the Laboratoire des Sciences du Climat, Gif-sur-Yvette, Paris, and suggesting the use of the Genevey et al. (2003) dataset. This work is supported by the Spanish "Plan Nacional de Investigación, Desarrollo e Innovación Tecnológica" (project REN2000-0896/ANT-COHIMAR) and the US National Science Foundation, Office of Polar Programs (OPP-award to Hamilton College). We also acknowledge support from the Spanish "Programa Hispano-Norteamericano de Cooperación Científica y Tecnológica", project 99120 (GEMARANT). GRC Geociències Marines of the University of Barcelona, Spain, is supported by "Generalitat de Catalunya" autonomous government through its excellence research groups program (ref. 2005 SGR-00152). V. Willmott benefited from a fellowship from the University of Barcelona.

References

Andrews, J.T., Domack, E.W., Cunningham, W.L., Leventer, A., Licht, K.J., Jull, A.J.T., DeMaster, D.J., Jennings, A.E., 1999. Problems and possible solutions concerning radiocarbon dating of surface marine sediments, Ross Sea, Antarctica. Quaternary Research 52, 206–216.

Berkman, P.A., Ku, T.-L., 1998. ^{226}Ra/Ba ratios for dating Holocene biogenic carbonates in the Southern Ocean: preliminary evidence from Antarctic coastal mollusc shells. Chemical Geology 144, 331–334.

Björck, S., Hakansson, H., Zale, R., Karlen, W., Jönsson, B.L., 1991a. A Late Holocene lake sediment sequence from Livingston Island, South Shetland Islands, with palaeoclimatic implications. Antarctic Science 3, 61–72.

Björck, S., Hjort, C., Ingólfsson, Ó., Skog, G., 1991b. Radiocarbon dates from the Antarctic Peninsula region—Problems and potential. In: Lowe, J.J. (Ed.), Quaternary Proceedings. Quaternary Research Association, Cambridge, pp. 55–65.

Björck, S., Sandgren, P., Zale, R., 1991c. Late Holocene tephrochronology of the northern Antarctic Peninsula. Quaternary Research 36, 322–328.

Brachfeld, S., Domack, E.W., Kissel, C., Laj, C., Leventer, A., Ishman, S.E., Gilbert, I.M., Camerlenghi, A., Eglinton, L.B., 2003. Holocene history of the Larsen-A Ice Shelf constrained by geomagnetic paleointensity dating. Geology 31, 749–752.

Canals, M., Urgeles, R., Calafat, A.M., 2000. Deep sea-floor evidence of past ice streams off the Antarctic Peninsula. Geology 28, 31–34.

Channell, J.E.T., Stoner, J.S., Hodell, D.A., Charles, C.D., 2000. Geomagnetic paleointensity for the last 100 kyr from the sub-antarctic South Atlantic: a tool for inter-hemispheric correlation. Earth and Planetary Science Letters 175, 145–160.

Domack, E.W., Jacobson, E.A., Shipp, S.S., Anderson, J.B., 1999. Late Pleistocene–Holocene retreat of the West Antarctic Ice-Sheet system in the Ross Sea: Part 2. Sedimentologic and stratigraphic signature. Geological Society of America Bulletin 111, 1517–1536.

Domack, E.W., Leventer, A., Dunbar, R., Taylor, F., Brachfeld, S., Sjunneskog, C., Party, O.L.S., 2001. Chronology of the Palmer Deep site, Antarctic Peninsula: a Holocene palaeoenvironmental reference for the circum-Antarctic. The Holocene 11 (9), 1–9.

Drake, A., 2002. Sediment analysis confirms a mid Holocene warming event in the Northwestern Weddell Sea, Antarctica. Unpublished B.A. thesis, Hamilton College.

Dunlop, D.J., 1997. Rock Magnetism. Cambridge Univ. Press, Cambridge.

Genevey, A., Gallet, Y., Margueron, J., 2003. Eight thousand years of geomagnetic field intensity variations in the eastern Mediterranean. Journal of Geophysical Research 108 (B5). doi:10.1029/2001JB001612.

Gordon, J.E., Harkness, D.D., 1992. Magnitude and geographic variation of the radiocarbon content in Antarctic marine life: implications for reservoir corrections in radiocarbon dating. Quaternary Science Reviews 11, 696–708.

Guyodo, Y., Valet, J.-P., 1996. Relative variations in geomagnetic intensity from sedimentary records: the past 200,000 years. Earth and Planetary Science Letters 143, 23–36.

Guyodo, Y., Valet, J.P., 1999. Global changes in intensity of the Earth's magnetic field during the past 800 kyr. Nature 399, 249–252.

Harden, S.L., DeMaster, D.J., Nittrouer, C.A., 1992. Developing sediment geochronologies for high-latitude continental shelf deposits: a radiochemical approach. Marine Geology 103, 69–97.

IOC, IHO, BODC, 2003. Centenary Edition of the GEBCO Digital Atlas. Published on CD-ROM on behalf of the Intergovernmental Oceanographic Commission and the International Hydrographic Organization as part of the General Bathymetric Chart of the Oceans. British Oceanographic Data Centre, Liverpool.

Isla, E., Masque, P., Palanques, A., Guillen, J., Puig, P., Sanchez-Cabeza, J.A., 2004. Sedimentation of biogenic constituents during the last century in western Bransfield and Gerlache Straits, Antarctica: a relation to currents, primary production, and sea floor relief. Marine Geology 209, 265–277.

Keller, R., Domack, E.W., Drake, A., 2003. Potential for tephrochronology of marine sediment cores from Bransfield Strait and the Northwestern Weddell Sea. XVI INQUA Congress. Reno, USA.

Laj, C., Kissel, C., Mazaud, A., Channell, J.E.T., Beer, J., 2000. North Atlantic palaeointensity stack since 75 ka (NAPIS-75) and the duration of the Laschamp event. Philosophical Transactions of the Royal Society London Series A 358, 1009–1025.

Laj, C., Kissel, C., Mazaud, A., Michel, E., Muscheler, R., Beer, J., 2002. Geomagnetic field intensity, North Atlantic Deep Water circulation and atmospheric $\Delta^{14}C$ during the last 50 kyr. Earth and Planetary Science Letters 200, 177–190.

Lichtenstein, S.J., Drake, A., Domack, E.W., Camerlenghi, A., Gilbert, I.M., Brachfeld, S., Leventer, A., 2002. Marine sediment cores from the northern Prince Gustav Channel: a record of the Holocene climatic optimum confirms trans-peninsula warmth ~6000 yr BP. Antarctic Peninsula Climate Variability: A Historical and Paleoenvironmental Perspective. Hamilton College, Clinton, NY.

Masque, P., Isla, E., Sanchez-Cabeza, J.A., Palanques, A., Bruach, J.M., Puig, P., Guillen, J., 2002. Sediment accumulation rates and carbon fluxes to bottom sediments at the Western Bransfield Strait (Antarctica). Deep Sea Research Part II: Topical Studies in Oceanography 49, 921–933.

Matthies, D., Mäusbacher, R., Storzer, D., 1990. Deception Island tephra: a stratigraphical marker for limnic and marine sediments in Bransfield Strait area, Antarctica. Zentralblatt für Geologie und Palontologie 1, 153–165.

Mazaud, A.S., M.A., Ezat, U., Pichon, J.J., Duprat, J., Laj, C., Kissel, C., Beaufort, L., Michel, E., Turon, J.L., 2002. Geomagnetic-assisted stratigraphy and sea surface temperature changes in core MD94-103 (Southern Indian Ocean): possible implications for North-South climatic relationships around H4. Earth and Planetary Science 201.

McMillan, D.G., Constable, C.G., Parker, R.L., 2002. Limitations on stratigraphic analyses due to incomplete age control and their relevance to sedimentary paleomagnetism. Earth and Planetary Science Letters 201, 509–523.

Morgenstern, U., Taylor, C.B., Parrat, Y., Gaggeler, H.W., Eichler, B., 1996. ^{32}Si in precipitation: evaluation of temporal and spatial variation and as dating tool for glacial ice. Earth and Planetary Science Letters 144, 289–296.

Paillard, D., Labeyrie, L., Yiou, P., 1996. Macintosh program performs time-series analysis. EOS 77, 379.

Palmer, A.S., van Ommen, T.D., Curran, M.A.J., Morgan, V., Souney, J.M., Mayewski, P.A., 2001. High-precision dating of volcanic events (A.D. 1301–1995) using ice cores from Law Dome, Antarctica. Journal of Geophysical Research 106, 28,089–28,095.

Peng, L., King, J.W., 1992. A Late Quaternary geomagnetic secular variation record from Lake Waiau, Hawaii, and the question of the Pacific nondipole low. Journal of Geophysical Research 97, 4407–4424.

Pope, P.G., Anderson, J.B., 1992. Late Quaternary glacial history of the northern Antarctic Peninsula's western continental shelf. In: Elliot, D.H. (Ed.), Evidence from the marine record, Contributions to Antarctic Research III, Antarctic Research Series. American Geophysical Union, Washington, DC, pp. 63–91.

Pudsey, C.J., Barker, P.F., Larter, R.D., 1994. Ice sheet retreat from the Antarctic Peninsula Shelf. Continental Shelf Research 14, 1647–1675.

Sagnotti, L., Macrí, P., Camerlenghi, A., Rebesco, M., 2001. Environmental magnetism of Antarctic Late Pleistocene sediments and interhemispheric correlation of climatic events. Earth and Planetary Science Letters 192, 65–80.

Smellie, J.L., 1999. The upper Cenozoic tephra record in the south polar region: a review. Global and Planetary Change 21, 51–70.

Stoner, J.S., Laj, C., Channell, J.E.T., Kissel, C., 2002. South Atlantic and North Atlantic geomagnetic paleointensity stacks (0–80 and ka): implications for inter-hemispheric correlation. Quaternary Science Reviews 21, 1141–1151.

St-Onge, G., Stoner, J.S., Hillaire-Marcel, C., 2003. Holocene paleomagnetic records from the St. Lawrence Estuary, eastern Canada: centennial- to millennial-scale geomagnetic modulation of cosmogenic isotopes. Earth and Planetary Science Letters 209, 113–130.

Tauxe, L., 1993. Sedimentary records of relative paleointensity of the geomagnetic field: theory and practice. Reviews of Geophysics 31, 319–354.

Tauxe, L., Wu, G., 1990. Normalized remanence in sediments of the western equatorial Pacific: relative paleointensity of the geomagnetic field. Journal of Geophysical Research B: Solid Earth 95, 12,337–12,350.

Van Beek, P., Reyss, J.-L., Paterne, M., Gersonde, R., van der Loeff, M.R., Kuhn, G., 2002. 226Ra in barite: absolute dating of Holocene Southern Ocean sediments and reconstruction of sea-surface reservoir ages. Geology 30, 731–734.

Willmott, V., Canals, M., Casamor, J.L., 2003. Retreat History of the Gerlache-Boyd Ice Stream, Northern Antarctic Peninsula: an ultra-high resolution acoustic study of the deglacial and post-glacial sediment drape. In: Domack, E.W., Leventer, A., Burnett, A., Bindschadler, R., Convey, P., Kirby, M.E. (Eds.), Antarctic Peninsula Climate Variability: a Historical and Paleoenvironmental Perspective. Antarctic Research Series. American Geophysical Union, Washington, DC, pp. 183–194.

Yang, S., Odah, H., Shaw, J., 2000. Variations in the geomagnetic dipole moment over the last 12000 years. Geophysical Journal International 140, 158–162.